

1. INTRODUCTION

One of the emerging approaches of urban planning is the use of underground spaces in urban development. With underground space possibilities, this strategy aims to alleviate space shortages and transportation concerns [1]. In such situations, population growth and city expansion have resulted in a shortage of space. Engineers are more likely to use underground spaces as a result of this. Construction of underground structures in urban areas, on the other hand, is dangerous, and all aspects of the careful design must be followed to reach the appropriate level of safety [2]. Metro tunnels and inner-city traffic tunnels are two of the most important underground places, and their construction demands additional excavations, which can worsen safety concerns [3]. The distance between two tunnels, the diameter of the tunnels, and the rigidity of their supporting system affect the amount of interaction between adjacent tunnels. As a result, choosing the proper excavation method and analyzing the behavior of the structure of the two tunnels and the surrounding land is essential and necessary to avoid possible damages [4]. Due to the inherent complexities of soil-tunnel interaction, analyzing the mechanical behaviors of tunnels and the surrounding land is a more significant challenge in adjacent tunnels than in other tunnels [5-6]. The acceptable deformation of the tunnel walls and working chest caused to the expansion of the plastic zone, which leads to an increase in existing settlements in the area, is one of the essential factors in the design and implementation of such projects [7].

Maadikhah used numerical modeling to analyze the effects of excavating the Tehran Metro Line 7 tunnel on the East Tehran sewage tunnel in a similar project. According to this study, the proximity of the subway tunnel to the sewage tunnel has increased the sewage tunnel's subsidence rate and caused stress [8]. Hosseini also analyzed the tunnel crossing at the intersection of Tehran Metro Lines 3 and 7. According to the results, surface subsidence has increased as the machine reaches the intersection and passes the end of the machine shield from the desired site [9]. Liu has analyzed the interaction between non-level cross tunnels in Sydney by excavating the existing tunnel supporting system by installing instruments [10]. Lai examined non-level cross tunnels with low intersection angles. According to data collected, the distortion of the primary tunnel caused by the excavation of the second tunnel, which passes diagonally under it, causes a torsional deformation in addition to a vertical settlement [11]. Lane's tunnel behavioral analysis caused tunnel crossing with a low intersection angle below it is another critical study in this subject. According to these studies, decreasing the angle of intersection between two non-level cross tunnels increases the level of asymmetric deformation in the existing tunnel [12]. On a larger scale, Zhang has analyzed the metro's twin tunnels. In this study, the effect of excavating a subway station on the twin tunnels above the station has been analyzed. [6]. Wang also used numerical and analytical methods to analyze the effects of excavating parallel tunnels on each other. The influence of the axial angle between the two tunnels and their size was studied in this case [13]. Afshani, like Wang, analyzed the excavation effect of parallel tunnels. However, the tunnels in this study have an elliptical cross-section [14].

In this research, the impact of new tunnel excavation on the supporting system of adjacent structures is studied. In order to study this effect, the distribution of bending moment, inductive stresses and shear force on the crown and piles of the Towhid tunnel has been modeled with the help of PLAXIS 3D.

2. MODELING GEOMETRY AND GEOTECHNICAL SPECIFICATIONS

The model's geometry made according to Figure 1 consists of a rectangular cube block with dimensions of length and width of 150 m and height of 67 m. Towhid tunnel is a double-arched tunnel with a width of 12.5 m and a height of 8.5 m. The final supporting system of this tunnel is made of reinforced concrete. The thickness of this supporting system is 1.2 m in the walls and 0.75 m in the crown. The load of the Towhid tunnel is transferred to the depths of the soil by three rows of piles. The piles in the central row are 4 m apart and have a diameter of 1.7 m, while the side piles are 2.5 m apart and have diameters of 0.8 m. In the study area, the overburden of the Towhid tunnel is 15 m.

The access gallery to the S7 station is also modeled with a width of 5.4 m and a height of 4.6 m. The initial supporting system of this gallery, which is responsible for the load transfer operation, is made of 30 cm of mixed mesh and shotcrete cover. This gallery has been excavated from top to bottom with the traditional drilling method.

Table 1 shows the values of geotechnical properties of the soils, and Table 2 shows the input parameters of Towhid tunnel structures and access gallery.

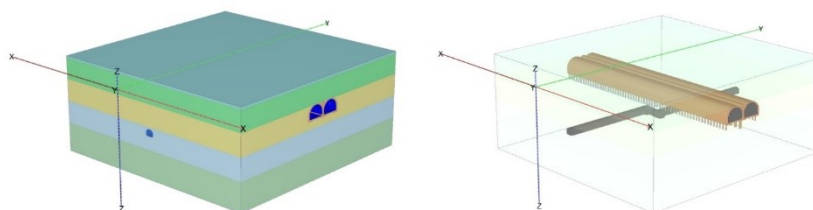


Figure 1: Modeling Geometry

Table 1: Geotechnical Parameters of Ground Layers

$K_0=1-\sin\phi$	Poisson ratio	Elastic modulus (KN/m ²)	Cohesion (KN/m ²)	Friction angle (degree)	Unsat density (KN/m ³)	Layer thickness (m)	Item
0.657	0.3	15e3	10	20	17.5	0-1.5	Layer 1
0.455	0.325	49e3	19.6	33	20.5	1.5-15.5	Layer 2
0.426	0.325	98e3	29.4	35	21.6	15.5-30.5	Layer 3
0.426	0.325	14.7e4	39.2	35	21.6	30.5-45.5	Layer 4
0.412	0.325	17.7e4	39.2	36	22.1	>45.5	Layer 5

Table 2: Structural Parameters of Towhid and Access Gallery

Poisson ratio	Elastic modulus (KN/m ²)	Density (KN/m ³)	Item
0.2	25.8e6	25	Final lining of Towhid tunnel
0.2	74.8e5	22.2	Central piles of Towhid tunnel
0.2	74.8e5	22.2	Side piles of Towhid tunnel
0.25	21.5e6	25	Initial lining of access gallery

Excavation and execution are divided into three parts in the 109-phase model. The first part is determining the environment's general conditions and distributing the area's soil properties. The second part consists of 33 phases in which the complete Towhid tunnel has been excavated. The third stage consists of 75 phases in which the access gallery excavation operation is performed. At the beginning of the third section, all deformations and displacements are considered to be zero in order to analyze only the impact of the access gallery excavation on the Towhid tunnel.

3. RESULTS ANALYSIS

To study the effect of access gallery excavation on the Towhid tunnel, the inductive stress curves on the tunnel crown and piles should be analyzed. The hypothetical north is supposed to be in the negative direction of the X-axis in the proposed results. Figure 2 shows the maximum bending moment distribution on the Towhid tunnel's east and west crowns, whereas Figure 3 shows the axial force distribution on both crowns.

The curves in Figure 2 show the maximum bending moment distribution before and after gallery excavation. According to this figure, the distribution of the bending moment in both cases has a uniform pattern. As seen in these curves, the structure has played great in the face of load applied by the surrounding ground.

After gallery excavation, the maximum bending moment for the western crown increased by 5.63 percent, from 1420 KNm/m to 1500 KNm/m. Furthermore, the maximum bending moment for the eastern crown before excavation began was 1430 KNm/m, which increased by 80 units to 1510 KNm/m after excavation completion. These amounts show that value increase to 5.59 percent.

Figure 3 also shows the distribution of maximum axial force on both crowns of the Towhid tunnel in two modes; before the excavation of the access gallery began and after it was completed. The force distribution on the two tunnel crowns shows relative symmetry, according to these curves. According to this figure, the amount of induced

axial force in the outer parts of the crown in the case before and after excavation the access gallery is more different. The maximum value for the western crown before the excavation of the access gallery is 9153 KN/m, and after the excavation of the gallery is completed, it is 9502 KN/m. These results show a 3.81 percent increase.

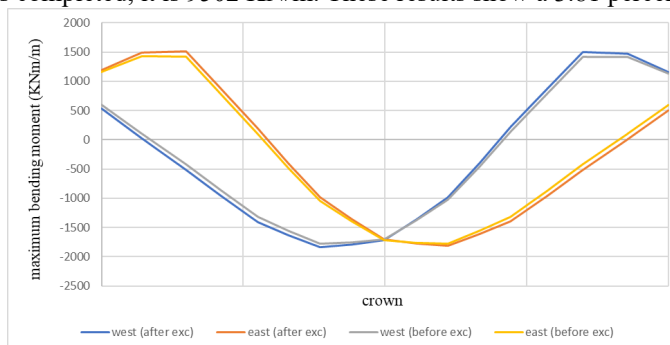


Figure 2: Maximum bending moment distribution on the crown of Towhid tunnel

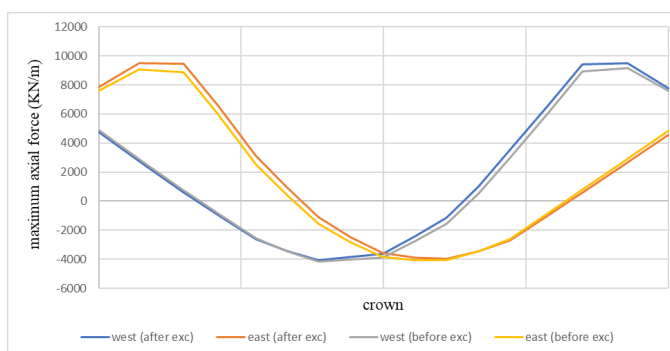


Figure 3: Maximum axial force distribution on the crown of Towhid tunnel

For the eastern tunnel crown, the amount of axial force increased by 422 units from 9086 to 9808 KN/m after the completion of excavation. These show 4.64 percent growth rate. Due to the more distance between the east tunnel and the access gallery, the crown of the east tunnel has increased more force. In this case, excavating the gallery will affect greater area and space. As a result, more of the surrounding ground is changed out of balance, and more load is placed on the eastern crown.

Figure 4 shows the maximum shear force distribution on the tunnel crown. According to the curves of this figure, the amount of shear force before and after excavation of the access gallery is not significantly different and at the extreme points are almost equal.

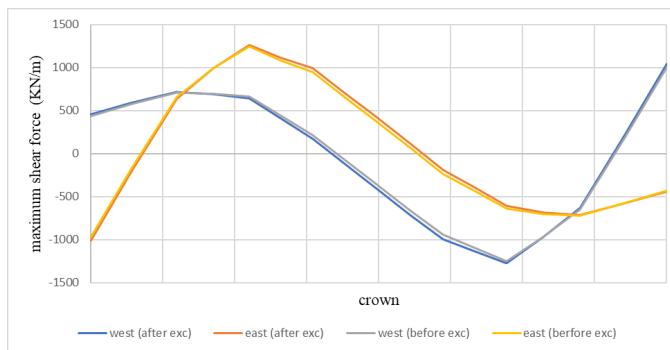


Figure 4: Maximum shear force distribution on the crown of Towhid tunnel

The Towhid tunnel piles are the closest structures to the gallery when excavating the access gallery from under the

Towhid tunnel. As a result, they expect a significant impact from the start of access gallery excavation. Figure 5 shows the distribution of the maximum bending moment along with the side pile of the west section above the access gallery route path in two modes: before excavation of the access gallery and after excavation of the access gallery. According to this figure, the bending moment is positive in the upper half of the pile in both cases and negative in the lower half of the pile.

The maximum bending moment has decreased by 5.17 percent from 290 to 275 KNm after completing the access gallery excavation. Most bending moments changes occurred in the upper half of the pile. Also, the bending moment in the lower half of the pile has decreased by 2.37 percent.

Figure 6 also shows the distribution of the maximum bending moment along with the side pile in the eastern part, which is located above the access gallery path. According to this figure, the maximum bending moment in the upper half of the pile after excavation has increased by ten units from -293 to -283 KNm. This rate of incremental change is equivalent to 3.41 percent. In addition, after excavation, the bending moment values in the lower half increased by 7.52 percent, from 67.5 to 72.58 KNm. Before and after excavating the access gallery, bending moment changes are more significant in the lower part.

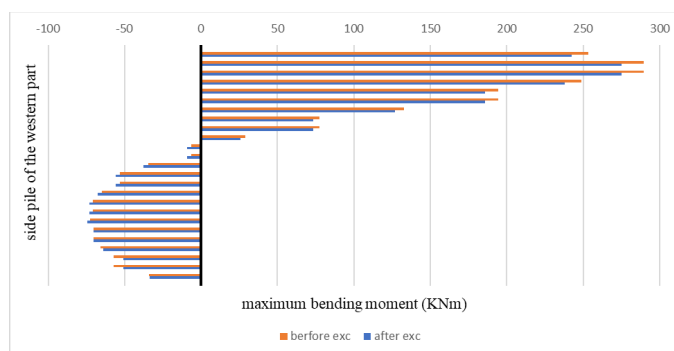


Figure 5: Maximum bending moment distribution on the western side pile

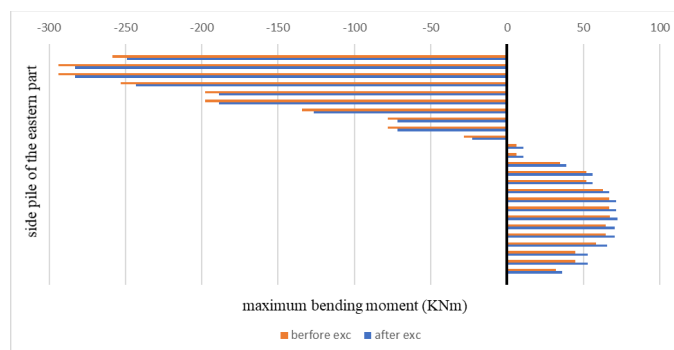


Figure 6: Maximum bending moment distribution on the eastern side pile

Figure 7 shows the distribution of the maximum bending moment on the Towhid tunnel's central pile, which is placed at the top of the access gallery path, both before and after the excavation of the access gallery. According to this figure, the direction of the bending moment on the pile has changed after the gallery excavation is completed. The bending moment in the upper half has increased from -28 KNm to 75 KNm in the opposite direction. These values show a 368 percent increase. The bending moment in the lower half of the pile has decreased from 13 KNm to 78 KNm per unit length in the opposite direction, with a 700 percent decrease in the amount of bending moment.

Figures 8, 9, and 10 show the distribution of axial force on the piles of the Towhid tunnel above the access gallery route path. According to Figure 8, with the completion of the excavation operation, the direction of the axial force in the western pile has changed. Before the excavation, the maximum axial force was -2123 KN, but after the completion of the access gallery excavation, it increased by 130 percent to 646 KN. As shown in figure 9, with the completion of the gallery excavation operation, the amount of axial force on the east pile has increased. The

maximum axial force after excavation is equal to -1086 KN, which shows an increase of 49.5 percent. According to Figure 10, the access of the axial force on the middle pile has increased after excavation. At maximum, the axial force increased by 152 percent from -4641 KN to 2429 KN.

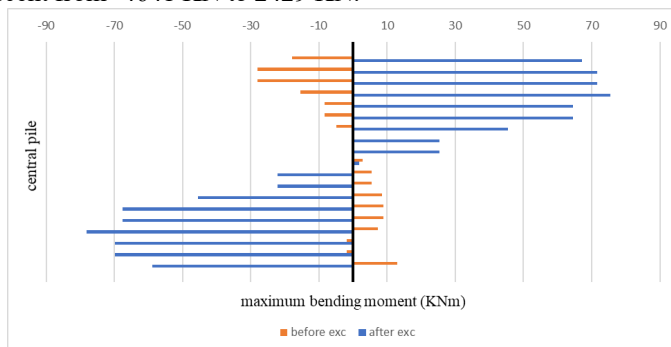


Figure 7: Maximum bending moment distribution on the central pile

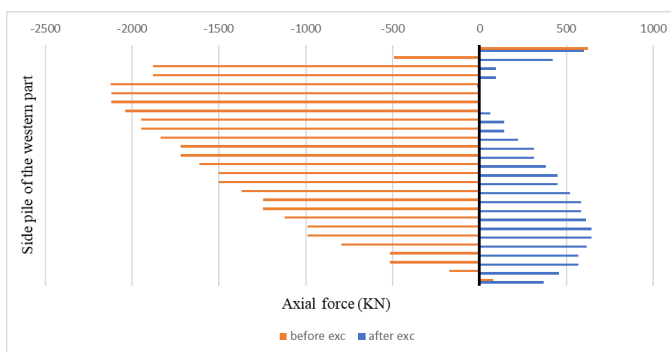


Figure 8: Axial force distribution on the western side pile

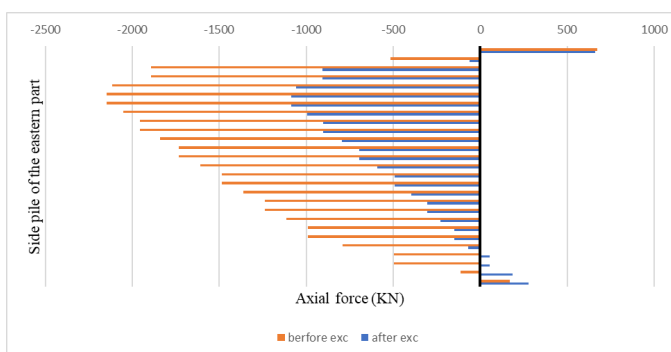


Figure 9: Axial force distribution on the eastern side pile

Figures 11, 12, and 13 show the pattern of shear force distribution on the piles both before and after the excavation of the access gallery. According to these three figures, the maximum shear force has occurred at the top of the piles.

For the western side pile, the shear force has reached -1734 KN after completing the access gallery excavation with an increase of 4 percent. For the eastern side pile, the maximum amount of shear force before the excavation is equal to 1847 KN, which after the completion of the gallery excavation, with a decrease of 3.62 percent, has reached 1780 KN.

4. CONCLUSION

This study analyzed the effect of new tunnel excavation on the supporting system of an adjacent existing structure using numerical modeling. The following results can be mentioned based on the studies:

- After excavation, the maximum bending moment on the western crown increased by 5.63 percent, reaching 1500 KNm/m. After excavation, the maximum amount of bending moment on the eastern crown has risen by 5.59 percent.
- The amount of maximum axial force in both crowns of the tunnel has increased after excavation. For the eastern crown, the amount of increase is equal to 422 KN/m, and for the western crown is equal to 349 KN/m. This difference in the final value of the maximum axial force after the excavation can be related to the longer distance between the Towhid tunnel and the gallery, which is longer on the eastern side, and the environment has changed more.

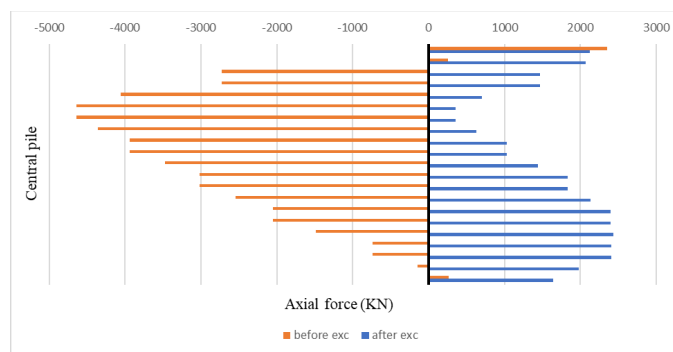


Figure 10: Axial force distribution on the central pile

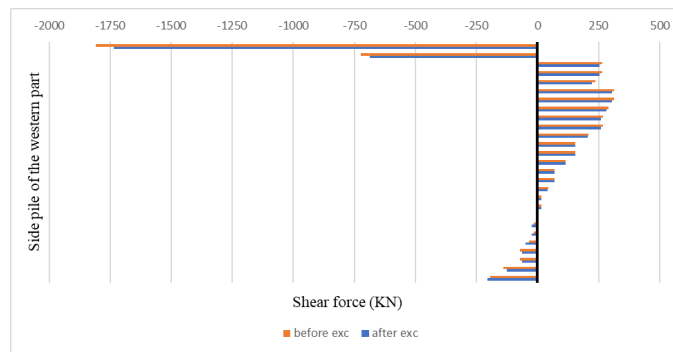


Figure 11: Shear force distribution on the western side pile

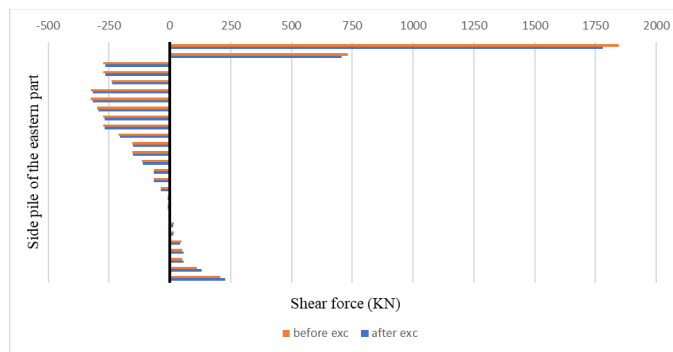


Figure 12: Shear force distribution on the eastern side pile

- The values of shear force in both parts of the crown of the Towhid tunnel are not significantly different and are equal in the maximum and minimum points.
- The maximum amount of changes in the bending moment of the piles has occurred in the upper part of them. After the gallery excavation, the amount of maximum bending moment in a pile above the axis line of the gallery located in the western row of Towhid tunnel was decreased by 5.17 percent. Also, for the eastern row pile, the amount of maximum bending moment after excavation has increased by 3.41 percent. The difference between the two modes in the central row pile is that the bending moment direction has changed after excavation.

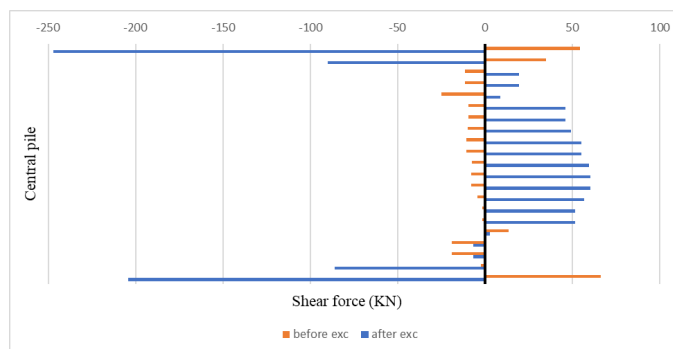


Figure 13: Shear force distribution on the central pile

- The amount of axial force on the piles under analysis has increased after the completion of excavation operations. Additionally, the shear force on the desired piles has undergone different changes. So that the side pile of the western part has increased by 4 percent, and the side pile of the eastern part has decreased by 3.62 percent.

REFERENCES

- [1] Ajorloo, H. and Ashtiani, M. (2016). Urban tunneling methods and related challenges, Tehran studies and planning center.
- [2] Faez, N. (2014). Numerical analysis of the interaction of parallel tunnels, MSc thesis, Zanjan university.
- [3] Guglielmetti, V. and Grasso, P. (2008). Mechanized Tunnelling in Urban Areas: design methodology and construction control, Taylor & Francis Group.
- [4] Asnavandi, M., Hasanloo, M., Hosseini, V., Mansouryar, M. (2012). studying the effect of excavating urban tunnels at the intersection of metro lines on adjacent structures using numerical methods, First National Conference on Civil Engineering and Development, Iran, February.
- [5] Xiang, L. (2019). Behavior of existing tunnel due to new tunnel construction below. Computers and Geotechnics. 110: 71-81.
- [6] Chengping, Z., Zhang, X., Fang, Q. (2018). Behaviors of existing twin subway tunnels due to new subway station excavation below in close vicinity. Tunnelling and Underground Space Technology. 81: 121-128.
- [7] Hosseinzadeh, M. (2014). Studying the effect of different soil parameters on the design of tunnels, MSc thesis, Khajeh nasir toosi university.
- [8] Maadikhah, A., Zare, Sh. (2012). Analyzing the effect of excavation of Tehran Metro Line 7 tunnel on the supporting system of Line 1 station in a non-level intersection using numerical modeling, The first asian conference and the ninth national tunnel conference, Iran.
- [9] Hosseini, S., Shahriar, K. (2012). Three-dimensional modeling of large and intersecting tunnels, Ninth national tunnel conference, Iran.
- [10] Liu, H., Small, Y., Carter, J., and Williams, D. (2009). Effects of tunnelling on existing support systems of perpendicularly crossing tunnels. Computers and Geotechnics. 36(5): 880-894.
- [11] Hongpeng, L., Haiwei, Z., Rui, C., Zuo, K., and Yang, L. (2020). Settlement behaviors of existing tunnel caused by obliquely undercrossing shield tunneling in close proximity with small intersection angle. Tunnelling and Underground Space Technology. 97: 103258.
- [12] Xing, L., Ren, C. (2019). Deformation behaviors of existing tunnels caused by shield tunneling undercrossing with oblique angle. Tunnelling and Underground Space Technology. 89: 78-90.
- [13] Wang, H. N., Gao, X., Wu, L., and Jiang, M. J. (2020). Analytical study on interaction between existing and new tunnels parallel excavated in semi-infinite viscoelastic ground. Computers and Geotechnics. 120: 103385.
- [14] Afshani, A., Akagi, H., and Konishi, S. (2020). Close construction effect and lining behavior during tunnel excavation with an elliptical cross-section. Soils and Foundations. 60(1): 28-44.